El Niño Enhances Snowline Rise and Ice Loss on the ~~World's Largest Tropical~~Quelccaya Ice Cap, Peru

Kara A. Lamantia[1,2], Laura J. Larocca[3], Lonnie G. Thompson[1,2], Bryan G. Mark[1,4]

[1] Byrd Polar and Climate Research Center, Ohio State University, Columbus, OH, USA
[2] School of Earth Sciences, Ohio State University, Columbus, OH, USA
[3] School of Ocean Futures, Arizona State University, Tempe, AZ, USA
[4] Department of Geography, Ohio State University, Columbus, OH, USA

Correspondence to: Kara A. Lamantia (lamantia.31.@osu.edu)

Abstract. Tropical glaciers ~~are essential water resources~~in the central Andes a~~re~~s vital water resources and crucial climate indicators, currently undergoing rapid retreat. However, understanding their vulnerability to the combined effects of persistent warming, short-term climate phenomena, and interannual fluctuations remains limited. Here we automate the mapping of key mass balance parameters on the Quelccaya Ice Cap (QIC) in Peru, one of the largest tropical ice caps~~, the world's largest tropical ice cap~~. Using Landsat's near-infrared (NIR) band, we analyze snow cover area (SCA) and total area (TA) and calculate the Accumulation Area Ratio (AAR) and Equilibrium Line Altitude (ELA) over nearly 40 years (1985-2023). Between 1985 and 2022, the QIC lost ~~46~~58% and ~3~~4~~7% of its SCA and TA, respectively. We show that the QIC's ~~loss~~ reduction in SCA and rise in ELA are exacerbated by El Niño events, which are strongly correlated to the preceding wet season's Ocean Niño Index (ONI). Further, ~~While variance testing indicates El Niño years have a strong impact on the SCA and La Niña years all record significant SCA~~ expansion in the QIC's SCA is observed during all La Niña years, ~~we observe that the QIC may be overwhelmed by anthropogenic climate impacts as it did not expand during~~except for the 2021-2022 La Niña. Although a singular event, this could suggest an inability for SCA recovery and accelerated decline into the future, driven primarily by anthropogenic warming.

~~with current and ongoing warming we expect the decline to continue through the next La Niña and into the future We observe lower levels of correlation to more recent El Niño events as anthropogenic climatic impacts overwhelm the natural forcing and continue to exacerbate loss at the QIC.~~

1 Introduction

Tropical glaciers are known to be especially sensitive to climate shifts (Kaser & Osmaston, 2002) and their accelerated decline has been ~~well-documented~~well-documented in recent decades (Bradley et al., 2006; Braun et al., 2019; Hanshaw & Bookhagen, 2014; Hugonnet et al., 2021; Pepin et al., 2015, 2022; Seehaus et al., 2020; Thompson et al., 2011, 2021; Vuille et al., 2015). In the low latitudes ~~and southern Andes~~, glaciers are projected to lose ~69-98% of their 2015 mass by 2100~~, respectively~~, depending on the emissions scenario~~s~~ (i.e., RCP2.6 and RCP 8.5, respectively; ~~(~~Rounce et al., 2023). The freezing level height

in the tropics is affected on an interannual basis by El Niño Southern Oscillation (ENSO) variations and follows the Multivariate ENSO Index (MEI) on a year-to-year basis (Bradley et al., 2009; Favier et al., 2004; Thompson, 2000; Vuille et al., 2000). The decline of the Quelccaya Ice Cap (QIC~~; the world's largest tropical ice cap~~; Fig. 1), located in the Cordillera Vilcanota (CV) range in the outer tropical region of the Andes, is one such concern with worst case (RCP8.5) projections suggesting the 'point of no return' ~~suggesting~~(i.e., the rise of the ELA above the summit)~~ its disappearance~~ as early as 2050 (Yarleque et al., 2018)~~, leading to the QIC's classification as~~leaving QIC a wasting ice field~~ instead of an ice cap~~, similar to Kilimanjaro. ~~ once, however due to its recent and~~is currently ~~now~~in (~~Kochtitzky et al., 2018~~)~~C~~Contemporary changes in the QIC's outlet glaciers have been monitored frequently (Brecher & Thompson, 1993) and contextualized within a longer, millennial-scale timeframe (e.g., Mark et al., 2002; Lamantia et al., 2023). For example, Mark et al. (2022) combine moraine chronology with digital topography to model deglaciation rates during the Last Glaciation and Holocene and find that~~(Brecher & Thompson, 1993) with~~ the QIC's most rapid ~~deglaciation computed to~~retreat has ~~have~~ occurred over ~~the most~~ recent centuries~~y modern retreat rates exceeding those reconstructed from Holocene moraines~~ (Mark et al., 2002). Further~~, evidence of the QIC's past fluctuations has recently been placed within a longer term context using~~ radiocarbon-dated plant remains from the QIC ice margin suggest~~ing~~ that the ice cap's retracted present-day ~~magnitude of retreat~~~~margin~~ extent has not occurred ~~since at least~~ in the last 7,000 years (Lamantia et al., 2023)~~ ago~~. In addition, the QIC's high-resolution ice-core records have proven invaluable for understanding ~~of~~ past climatic and environmental variability in the region (Thompson, 2000; Thompson et al., 1985, 2013, 2017, 2021). Thus, the ongoing loss of tropical glaciers will not only impact local communities that depend on glacial meltwater but has implications for the preservation of long-term climate records, essential for assessing the rate and magnitude of current changes (Thompson et al., 2021).

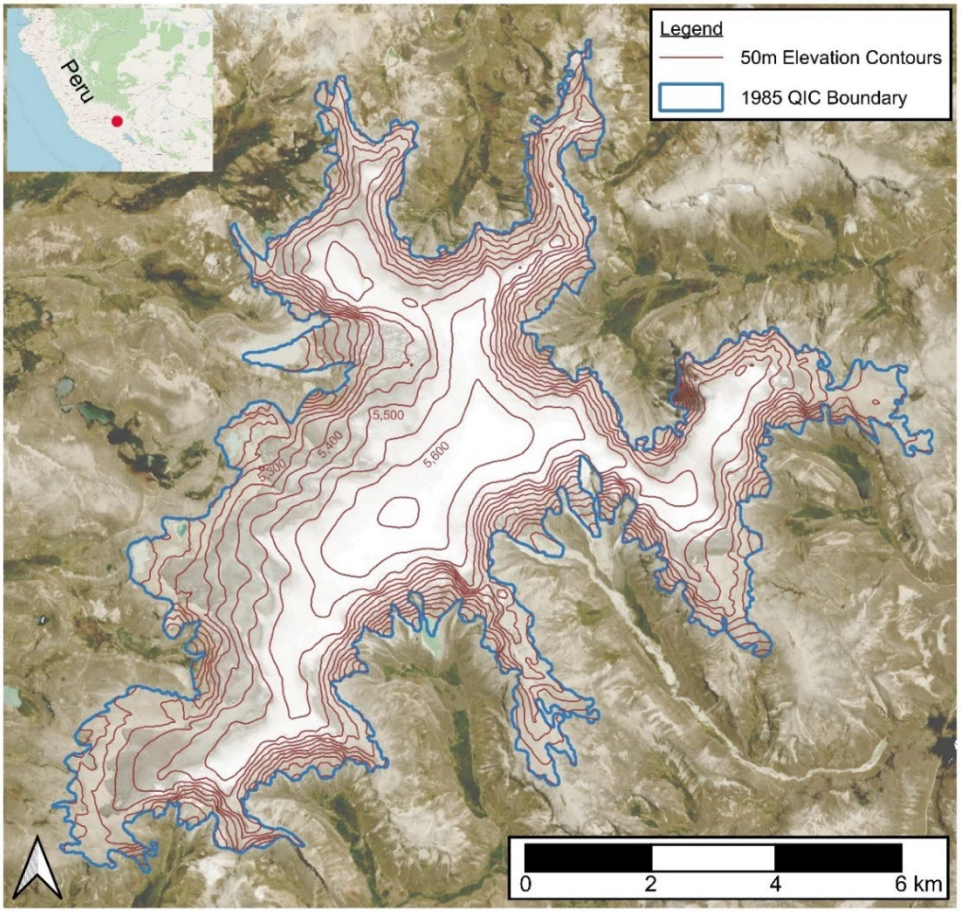

Figure 1: Aerial view of the Quelccaya Ice Cap (13°56'S; 70°50'W) from October 11, 2023. The summit of the QIC reaches 5,670 m a.s.l with a handful of outlet glaciers to the west and a steep-sided eastern portion. Base Imagery was obtained from Planet Labs Dove Satellite with 3-meter resolution and inset (top left) was obtained from the OpenStreetMap database (© OpenStreetMap contributors 2023. Distributed under the Open Data Commons Open Database License (ODbL) v1.0.)

In the tropics, there is no seasonal snow cover beyond the glacierized area that would provide an additional buffer to the ice cap's decline (Vuille et al., 2018). Quelccaya's snowfall is largely controlled by the South American Summer Monsoon (SAMS) with the snowfall peak in December and moisture transport from the Amazon is influenced by ENSO variations (J. V. Hurley et al., 2015). ~~The southern wet outer tropics are climatically controlled by fluctuations in the Intertropical Convergence Zone (ITCZ) and glaciers such as the QIC have enhanced temperature sensitivity relative to those in the dry outer tropics (Veettil et al., 2017).~~ There has been no significant change in precipitation around the QIC over the last fifty years, with 10% of stations in the CV recording only a slight decrease in rainfall (Casimiro et al., 2013). However, ~~but~~ ice core records from the QIC core reveal the net accumulation in the region has been above average for the last century (Thompson L.G., 2017). In the Peruvian Amazon–Andes basin, ~~The average~~ mean annual temperature has increased by ~0.09°C per decade over the last sixty years, while ~~with~~maximum ~~the~~ summer temperature time series in the Andes show an even higher magnitude

trend (0.15°C per decade; ~~months recording a higher magnitude increase in maximum~~ summer ~~temperature (~~Casimiro et al., 2013). Additionally, ~~and~~ ice cores from multiple locations in Peru ~~recording~~ document~~ing~~ thi~~s~~e accelerating enrichment (Thompson, 2017; Thompson et al., 2013). Nearby mountain ranges such as the Cordillera Blanca and Real have experienced an increase in the freezing level height (FLH) by 160 m over the last five and a half decades with implications for not only where snow can survive and accumulate (Bradley et al., 2009; Schauwecker et al., 2014; Seehaus et al., 2020) but also increased albedo in the ablation zone influenced by a rise of the rain/snow line (Rabatel et al., 2013). High-resolution ice core records show that the QIC is an excellent recorder of ~~the~~ El Niño ~~and La Niña~~ events that create elevated sea surface temperatures (SSTs) in the Eastern Pacific Ocean, recording years of strong El Niño events with isotopically enriched $\delta^{18}O$ (Thompson et al., 2011, 2017). Alongside these ice core records, the QIC's contemporary and past margins have ~~has~~ been monitored and reconstructed, but its ~~has yet to be evaluated for ice loss~~sensitivity and response to multiple short-term climate phenomena over recent decades have yet to be extensively evaluated ~~that may play a role in its current decline~~. Thus, the QIC is an ideal setting to assess the combined effects of sustained warming and short-term climate variations, such as ENSO, on tropical glacier vulnerability.

Since routine ground-based measurements in a remote location such as south-central Peru are difficult to maintain, using satellite imagery to estimate the Equilibrium Line Altitude (ELA) has become a viable solution for long-term glacier monitoring. Previous studies have shown that the end of dry season (September) location of the snowline altitude (SLA) can act as a proxy for the ELA and ultimately be used to infer the mass balance of a glacier or ice cap (Fang et al., 2011; Hu et al., 2020; Liu et al., 2021; Racoviteanu et al., 2019). Initial studies in the Andes involved a manual assessment of the Artesonraju and Zongo glaciers via Landsat and SPOT imagery compared against field measurements (Rabatel et al., 2012). Yarleque et al., (2018) most recently analyzed the QIC's response to warming scenarios based on the FLH/ELA relationship and future ELA projections. Here, we ~~use~~employ cloud-based analysis of satellite imagery ~~a suite of imagery spanning 1985 to 2023~~ to assess the QIC at the end of the dry season between 1985 and 2023 ~~through a cloud based analysis of satellite imagery~~. We automate not only the detection of the snow-covered area (SCA) and total area (TA), but also the calculation of the accumulation area ratio (AAR), the median elevation of the SCA, and the SLA as a proxy for the ELA. Changes to the ELA, SCA, and AAR are analyzed alongside ERA5—Land Reanalysis Climate Data from the European Centre for Medium Weather Range Weather Forecast (ECMWF) including total precipitation and surface temperature as well as multiple ENSO Indices including the MEI, the Ocean Niño Index (ONI), and the Southern Oscillation Index (SOI). We ~~additionally~~ focus on the strongest most recent El Niño events (1998, 2016, and~~&~~ 2023) and the QIC's response to these short-term climate anomalies.

2 Methods

2.1 Current Analysis Techniques

Manual snowline tracing is often limited to high quality imagery to ~~determine~~iscern between snow ~~versus~~ and ice ~~presence~~. However, r~~R~~ecent advances in image analysis have ~~included~~ allowed for the automation of snowline detection via satellite imagery~~as often manual tracing is limited to higher quality imagery to determine snow versus ice presence~~. Typically, a suite of images, often from Landsat satellites, are paired with one or more Digital Elevation Models (DEMs) and a glacier outline ~~from the beginning of~~within the temporal scale of interest (Li et al., 2022). From there, a variety of thresholds are evaluated and set for the area of interest to separate snow from ice, and extract the position of the transition ~~with the SLA extracted from automated calculations to be used as the ELA~~ (Racoviteanu et al., 2019) ~~or manual tracing of outputs (Liu et al., 2021)~~. There are challenges in this process including the adjustment of~~ing~~ surface reflectance ~~from the~~for varying topographiesy~~,~~, occurrence of patchy snow cover on the~~a~~ glacier surface, and highly variable atmospheric conditions that require the algorithm to be ~~adjusted to~~customized for the location of interest (Racoviteanu et al., 2019). Previous studies on Andean glaciers have used ~~included~~ a handful of techniques to extract the location of the snowline and to overcome some of the aforementioned challenges, ~~including satellite imagery analysis and~~ spectral mixing analysis ~~from the Landsat short wave infrared (SWIR) and near infrared (NIR) bands (Klein & Isacks, 1999)~~, simple ~~as well as satellite imagery~~ band ratios and filtering, hillshade mask shadow removal, and manual editing (Hanshaw & Bookhagen, 2014; Klein & Isacks, 1999). Here we ~~a~~ implement an automated approach that employs~~ing~~ a~~the necessary~~ topographic correction, ~~and~~ followed by ~~image~~ segmentation ~~via the OTSU method~~ of the NIR band via the OTSU method, which we describe in further detail in section 2.3, below.

2.2 Data Collection

To automate the SCA detection and ELA calculation, the following data inputs were required: an annual satellite image, a DEM, and the 1985 outline of the QIC. Using the Google Earth Engine platform (GEE) we selected annual Landsat images as close as possible to September 15th~~st~~ with clear visibility of the QIC from 1985 to 2023 (Table S1). ~~September 1~~Mid to end September marks the end of the dry season in the CV, which enabled analysis of the ice cap without extraneous snowfall around the perimeter. Imagery from each year was on average ±23 days within the target date and was manually inspected to ensure no recent snowfall events occurred. ~~Additionally, I~~if September imagery was not available, October and November images were collected, and if imagery was still not available August and July were collected with the intention to collect the closest~~best~~ to end of dry season conditions at the QIC. No images were used ~~and were not used~~ if a recent snowfall event was evident. Sentinel-2 imagery was used in 2021 and 2023, due to a lack of cloudless images from Landsat 8/9. ~~As one of our aims was to analyze the 2023 El Niño event, a separate~~Separate scripts were adapted for each satellite (i.e., Landsat or Sentinel-2 ~~set of~~) ~~imagery~~. ~~script was adapted for the higher resolution and alternate detail of Sentinel-2 processing.~~ We note that the 2023 results are not included in our initial analysis of QIC's ELA change as it is part of an incomplete El Niño event. No imagery was collected for the years 1987, 1994~~3~~, 2004~~2~~, ~~and~~ 2012, and 2018 due to high cloud cover and/or visible snowfall

events. We used two DEMs to~~usage~~ account~~ed~~ for changes in ice elevation over time and any down wasting of the QIC. I~~, and~~ ~~i~~nitially the NASADEM, created from the Shuttle Radar Topography Missions (SRTM), was implemented from 1985 to 2005. Post 2005, the COP30 DEM, released in 2010, was implemented following an assessment of surface ~~difference~~ differences in both DEMs between 2005 to 2015. Additionally, throughout and following the two largest El Niño events (1997-1999 and~~&~~ 2015-2017), ~~16 and 18~~ multiple images (16 and 18, respectively) ~~from June of the first year to November of the last year, respectively,~~ were collected, ~~from June of the first year to November of the last year,~~ to assess short-term change and response of the QIC to El Niño events.

2.3 Satellite Analysis for Snow Cover Area

To begin, the least cloudy image from the ~~end dry season~~ target year closest to the end of dry season is clipped to the region of interest (ROI), the delineated QIC boundary (Step 1; Fig. S1). Pre-processing of each image included calculating the slope and aspect of the ROI from the DEM (Step 2). We ~~then~~ implemented the Ekstrand Correction (Ekstrand, 1996) to account for topographic effects such as shadowing~~,~~ due to differences in~~t~~ sun elevation ~~s~~ and incidence angle (Step 3) rather than~~.~~ ~~illumination condition, which for the detection of the same features under different sunlight conditions (Step 2; Martín-Ortega et al., 2020). We use the Minnaert Correction (Ge et al., 2008), which assumes the reflectance of a surface is proportional to the cosine of the angle of incidence. Both are used to topographically correct for variability of observed reflectance and apply such to the selected annual image (Step 3; Ge et al., 2008). The QIC's low sloping topography works well with this method instead of~~ a pixel-based Minnaert Correction method (Ge et al., 2008) which resulted~~and set band coefficients as it results~~ in ~~the~~ the over-correction of the steeper eastern side of the QIC. ~~is an excellent case study for this method as the low-sloping topography does not create as many shadows as a steep mountain glacier.~~ To delineate the snow cover area (SCA), the NIR band was assessed with an image segmentation algorithm, the OTSU method (Gaddam et al., 2022). This results in ~~. The NIR band records~~ a bimodal frequency histogram where an ~~of snow and ice and the OTSU method is designed to~~ automatically detect~~ed the~~ threshold separates snow from ice (Step 4; Fig. S2). Once calculated, it is applied to the NIR band to create a binary mask of snow and ice (Step 4). The annual image and DEM are then clipped to the snow mask creating the SCA, and the DEM data is extracted (Step 5). Following this, ~~and~~ the SCA is calculated based on the number of pixels and image resolution, and the median elevation of the SCA is determined~~are calculated~~. SCAs are exported to shapefiles and the DEM data is exported as a histogram in 50-meter elevation bins (Step 6).

2.3 Calculation of Total Area, AAR, and ELA, and Uncertainty

As the SLA is a proxy for the ELA, we will use the term ELA from this point forward. In pursuit of the ELA, we calculated the Accumulation Area Ratio (AAR). The AAR is defined as: AAR = Ac/(Ac +Ab) where Ac is the accumulation area, Ab is the ice covered area, and Ac + Ab is the total area (TA) (Meier, 1962). In this case, Ac is the SCA and Ac+Ab is the TA (both ice and~~&~~ snow). To calculate the TA, we automated the calculation of the Normalized Difference Snow Index (NDSI), which leverages the reflectance of snow and ice in the green and SWIR spectra compared to other land cover types. The NDSI is

calculated by the following equation: NDSI $= (\rho_G - \rho_{SWIR})/(\rho_G + \rho_{SWIR})$, where ρ_G and ρ_{SWIR} are the reflectance of the green and shortwave infrared bands, respectively (Dozier, 1989; Hall & Riggs, 2007). We used the same OTSU thresholding method to calculate the NDSI threshold, typically set around 0.4 (Dozier, 1989; Hall & Riggs, 2007; Sankey et al., 2015). The number of snow- and ice-covered pixels is multiplied by the appropriate pixel resolution to obtain the TA. By applying the threshold to each image, we obtained a binary image of snow and~~& /~~ice versus land cover~~neither~~ and used this to calculate the TA (Step 7). The AAR is calculated by dividing the SCA by the TA (Step 8). The ELA is calculated using the DEM and the AAR by taking the 1 – AAR percentile of all elevations in the TA (Step 9: Fig. S3). For example, if the AAR is 0.8, we assume the ELA is located at the 20th percentile of elevations in the TA. In summary, for each image analyzed, we obtained the SCA, the median elevation, the TA, the AAR, and the ELA. Calculated results for the SCA and TA via our automated methods are in good ~~robust~~ agreement with ~~seven~~ manual digitizations ~~(of the ELA SCA resulting in an error of SCA within~~within ±3%~~) of the automated SCA and TA calculations~~. Other studies have shown ~~manual and~~ automated detection of snowlines produce~~s~~ similar results to manual digitization and low level of error (Hanshaw & Bookhagen, 2014) with automated detection being preferable to manual ~~,~~as repetition is simpler and any error is likely to be more consistent (Paul et al., 2013).

2.4 Renanalysis Data and ENSO Correlation

To ~~observe~~compare the QIC's SCA and ELA ~~alongside~~ with climate, ~~ic variables~~ we used daily and monthly averaged ~~data from the~~ ERA5~~—~~Land Reanalysis Climate Data from the European Centre for Medium~~-~~ ~~Weather~~ Range Weather Forecasts (ECMWF), including total precipitation and ~~surface~~ 550mb temperature. Initially, we divided the data into wet (October to April) and dry (May to September) seasons based on precipitation records and past literature (Kaser & Osmaston, 2002; Veettil et al., 2017). To observe changes in climate at the QIC over time we calculated the average precipitation and temperature in five-year intervals, and the ~~number of~~ average number of days above and below freezing for each season from 1985 to 2023. Finally, t~~T~~o ~~analyze~~ assess the QIC's interannual response to climatic anomalies we paired detrended ELA, SCA, and median elevation with the MEI, SOI, and ONI indices for correlation. As such, the variables for each year were correlated with the preceding months' indices~~, for~~ one year before the annual September observation date.

3 Results

3.1 Ice Loss and Multi-Decadal Climate Trends

Over the observation period (1985 to~~and~~ 2022), the QIC lost ~347% of its TA and ~5846% of its SCA (1985: TA=~598.76 km^2, SCA=~46.38 km^2; 2022: TA=~369.67 km^2, SCA=~~25.3~~19.7 km^2~~; (~~Table S2). ~~Average loss B~~between the first and last five ~~observed~~ years of observation, the QIC's ~~and the last five recorded an~~ SCA and TA declined by~~of~~ ~38% and ~~the TA by~~ ~29%, respectively.~~.~~ This ~~SCA~~ TA loss is concurrent with a retreat of the ~~TA~~ SCA to higher elevations (Fig. 2). We observed a ~~168~~ 209 m and ~~84~~ 112 m rise of the ELA and median elevation of the SCA, respectively. In 1985, 90% of the SCA existed above 5,250 m a.s.l., and in 2021, 90% of the SCA shifted to elevations above 5,350 m a.s.l. Further, ~~, and~~by 2022, 90% of

the SCA shifted even higher, to elevations above 5,350 400 m a.s.l. On average, tThe SCA and TA record an average loss ofdecreased by ~0.72 km^2 and ~0.59 km^2 per year, with an average yearly ELA rise of ~5.65m. On averageL, linear regression models suggest a loss of 0.3947±0.09 km^2 yr^{-1} (R^2=0.3644, p<0.001) in the QIC's SCA; an average loss of 0.4948±0.023 km^2 yr^{-1} (R^2=0.9389, p<0.001) in the QIC's TA; and an average rise of 2.963.61±0.759 m yr^{-1} (R^2=0.3240, p<0.001) in the QIC's ELA. However, the removal of the three largest El Niño influenced years (1998, 2016, and 2023) indicate indicatesresulted ined slower average losses in QIC's SCA and TA, and a slower average rise in QIC's ELA: -0.3642±0.077 km^2 yr^{-1} (R^2=0.580, p<0.001); -0.47±0.03 km^2 yr^{-1} (R^2=0.89, p<0.001); and +2.723.25±0.59 64 m yr^{-1} (R^2=0.472, p<0.001), respectively (Table S3). The QIC's average AAR (minus not including El Niño and La Niña years) is 0.74 throughout over the study period. Conversely, during, with the strongest El Niño years (1998, 2016, and 2023) the QIC's AAR was (0.320, 0.4501, and& 0.522, respectively) and during the strongest La Niña years (1999 and 2011) the QIC's AAR was (0.83, and 0.82), as the exceptions. If we consider the 2023 El Niño, between 1985 to 2023, we observed a 60% decline in the QIC's SCA in just under 40 years (Fig. 4). Our measured variables show significant correlation to each other. For example, we find a strong positive correlation between the median elevation and the ELA (0.98), a strong negative correlation between the ELA and the SCA (0.98) and a strong positive correlation between the SCA and AAR (0.84, Table S4).

The QIC's Ddaily and monthly variations recorded atby the QIC summit and bottom margin weather stations from Bradley et al., (2009) are well correlated with the ERA5 surface 550mb temperature dataset, which was analyzed used to determine changes in meteorological temperaturevariables through the observation period. Analysis of the ERA5 Between the first and last five years in our observational period, surface the reanalysistemperature data records recorded a 0.60°C increase in wet season (October-April) temperature and ~46% of the wet season (October – April) and ~11% of the dry season (May – September) with mean daily temperatures above 0°C. Tthe average temperature of the first five and last five years a show an increaseincreasing of 0.5960°C in the wet season (October – April) and1.124°C increase in the dry season (May – September) temperature. Similarly, the number of days above 0°C rose from 321% to 506% in the wet season and from 50.5% to 178% in the dry season betweenover the first five and last five years. These results are consistent with previous studies discussing that suggest a ~0.1°C/decade rise in upper air temperature, and a rise in the height of the freezing levelline (~45 m between 1977-2007) in the tropics near the QIC (Bradley et al., 2009; Vuille et al., 2008). We observe no significant change in a linear regression for precipitation in both the wet and dry seasons (wet: R^2=0.02, p=0.05; dry: R^2=0.03, p=0.01) with 73% of the precipitation occurring during the wet season.

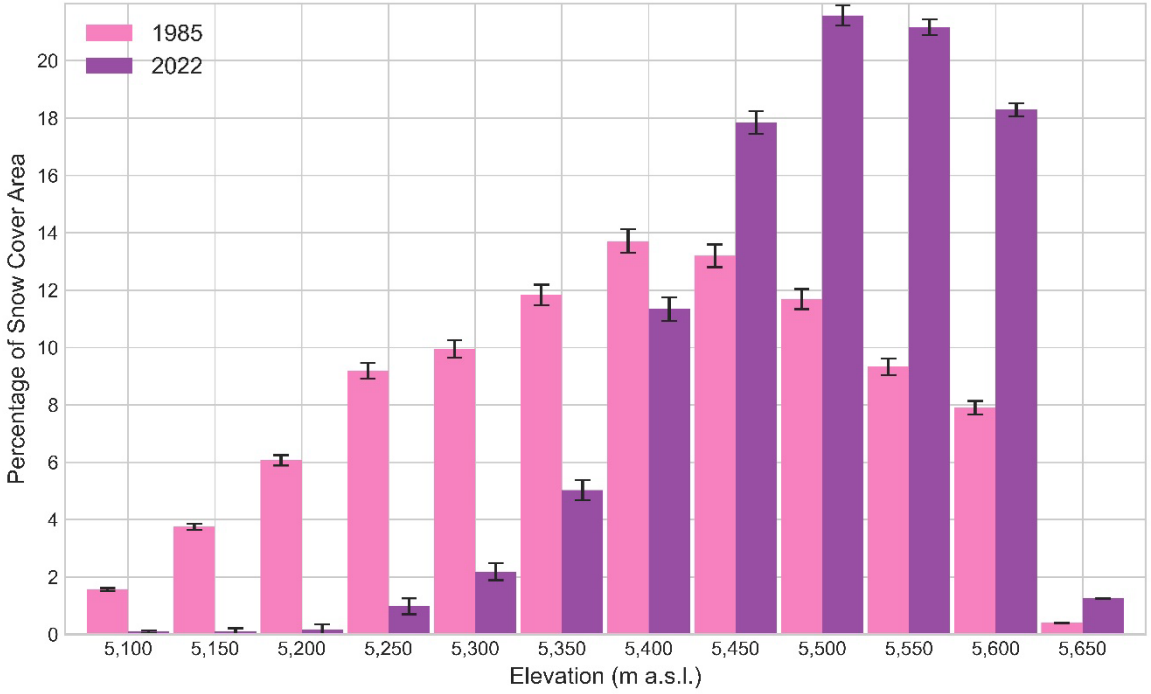

Figure 2: Percentage of snow cover area (SCA) in 50-meter elevation bins, demonstrating the shift to higher elevations.

3.2 QIC Response to Short-Term Climate Phenomena

The strongest El Niño events (1998, 2016, and 2023) coincide with a large decrease in the QIC's SCA. We observed a ~~63~~59% reduction~~loss~~ in SCA from 1997 to 1998 and a ~~40~~48% reduction ~~loss~~ from 2015 to 2016. In 1999, a rebound of the SCA was observed back to 1997 conditions however, in 2017 the SCA only ~~reaches~~ reached about 7~~0~~0% of its 2015 value (~32km^2) following the 2016 El Niño (Fig. 3). A small increase in the SCA is observed in 2019 (no imagery was available for 2018), however, to date the SCA has not~~ever~~ returned to its pre-El Niño 2015 ~~coverage~~extent and has continued to decline ~~up~~ through 2022. ~~full rebound in the SCA is not observed until two years following the event, in 2018.~~ To better determine ~~the patterns~~QIC changes during the El Niño events, high frequency sampling was conducted around the complete El Niño events, consisting of 16 and 18 images collected between 1997~~—~~1999 and 2015~~—~~2017, respectively. In both cases, the lowest SCA during El Niño is observed in the annual mid-~~-~~September measurement, with a steady decline occurring from the prior year's September measurement over the three consecutive years. In addition, correlation between the monthly ELA and monthly ONI index during the two El Niño events (1997-1999 and 2015-2017) are 0.68 and 0.26, respectively. The ~~1997 to 1998~~ QIC's AAR decreased~~rops~~ from 0.7~~1~~5 to 0.3~~1~~0 from 1997 to 1998 and from 0.76 to 0.41 from 2015 to 2016. ~~from 0.786 to 0.451.~~ During these El Niño events, ~~noticeable spikes are recorded in~~ ERA5 ~~temperature records~~data ~~recorded~~shows increased air temperatures while precipitation patterns and magnitude remain largely unchanged. For instance, during the dry season from

1997 to 1998 there is a 1.35°C increase in temperature and a change in~~of~~ total precipitation ~~under~~ of less than 0.025~~5~~ meters. Additionally, ~~If we fit~~ linear regression models for~~the~~ ELA and SCA that ~~to linear regression~~ include ~~model with~~ El Niño ~~years~~ as a binary predictor (i.e., yes or no)~~,~~ improve the~~the~~ R^2 values~~coefficients~~ ~~for the ELA and SCA~~ from 0.39 to ~~(R^2~~ =0.67 (~~,~~ p<0.001) and~~; &~~ 0.44 to ~~R^2=~~0.6772 (~~,~~p<0.001), respectively ~~improve with statistically significant values~~. ~~However~~Conversely, the R^2 value ~~TA coefficient~~ for the model predicting TA does not improve with the inclusion of the binary predictor~~s (R^2=0.903, p=0.73<0.001)~~. A~~a~~n analysis of variance ~~testing~~ (ANOVA) with a post hoc test ~~records~~ shows a significant difference in the mean SCA and ELA ~~from~~ between El Niño and~~to~~ neutral ~~conditions~~ years, ~~as well as~~nd in~~and~~ in the AAR between El Niño and~~to~~ neutral years and between El Niño to La Niña years (Fig S4~~1~~). There is no significant~~tee~~ difference in the mean TA ~~TA does not record any significant differencet within~~between El Niño, La Niña, and~~to~~ neutral ~~conditions~~ years (Table S4~~5~~). As the 2023 measurements occur during an ongoing El Niño event, we initially ~~complied~~ compiled data from 1985 to 2022 and report~~ed~~ the 2023 data as an additional insight into the effects of El Niño ~~events~~ on the QIC. If we consider the 2023 El Niño, between 1985 to 2023, we observed a 61% decline in the QIC's SCA in just under 40 years (Fig. 4). The QIC's SCA ~~observed~~ during the onset of the 2023 El Niño is ~17.97 km^2~~__~~, a ~~25~~9% loss compared to that of 2022. The 2023 AAR is ~~calculated at~~ 0.53~~2~~, well below the average (i.e. 0.74), and f~~. F~~rom 2022 to 2023, we observed a ~~31~~ 15 m and 8~~28~~ m rise of the ELA and median elevation ~~with 90% of the SCA existing over 5,400 m a.s.l. as opposed to 5,350 m a.sl. in 2022~~. ~~We intend to continue to monitor the QIC to determine the continued effects of the El Niño event and any possible rebound that could occur in 2024.~~

ENSO indices ~~were~~ are most strongly correlated with the QIC's ELA, SCA, and median elevation as they best represent the changing ice distribution and mass. We evaluated all three previously mentioned ENSO indices but have chosen to discuss the ONI as it presented the clearest patterns between ENSO and the assessed QIC variables (Table S5~~6~~). The ONI is measured as sea surface temperature (SST) anomalies in the Niño 3.4 zone (5˚N - 5˚S and~~&~~ 120˚W – 170˚W) and is ~~mostly~~ used to define El Niño and La Niña events. The ONI is most strongly correlated to the median elevation (~~Table 1~~Fig. 5) with a Pearson coefficient from the preceding April back through the previous September ranging from 0.~~489~~ 46 to 0.~~644~~ 61 (P<0.05). The ONI and ELA are similarly positively correlated (0.41 to 0.58 April-September), while ~~nd~~the ONI index and SCA exhibit a ~~median elevation recorded~~ negative correlation of similar strength ~~a similar pattern with the prior wet season (March~~ April through September (-0.44 to -0.60). ~~recording the highest correlations (0.517 41 to 0.64458). The SCA recorded a similar pattern through a negative correlation from the prior wet season (0.555 44 to 0.6041).~~

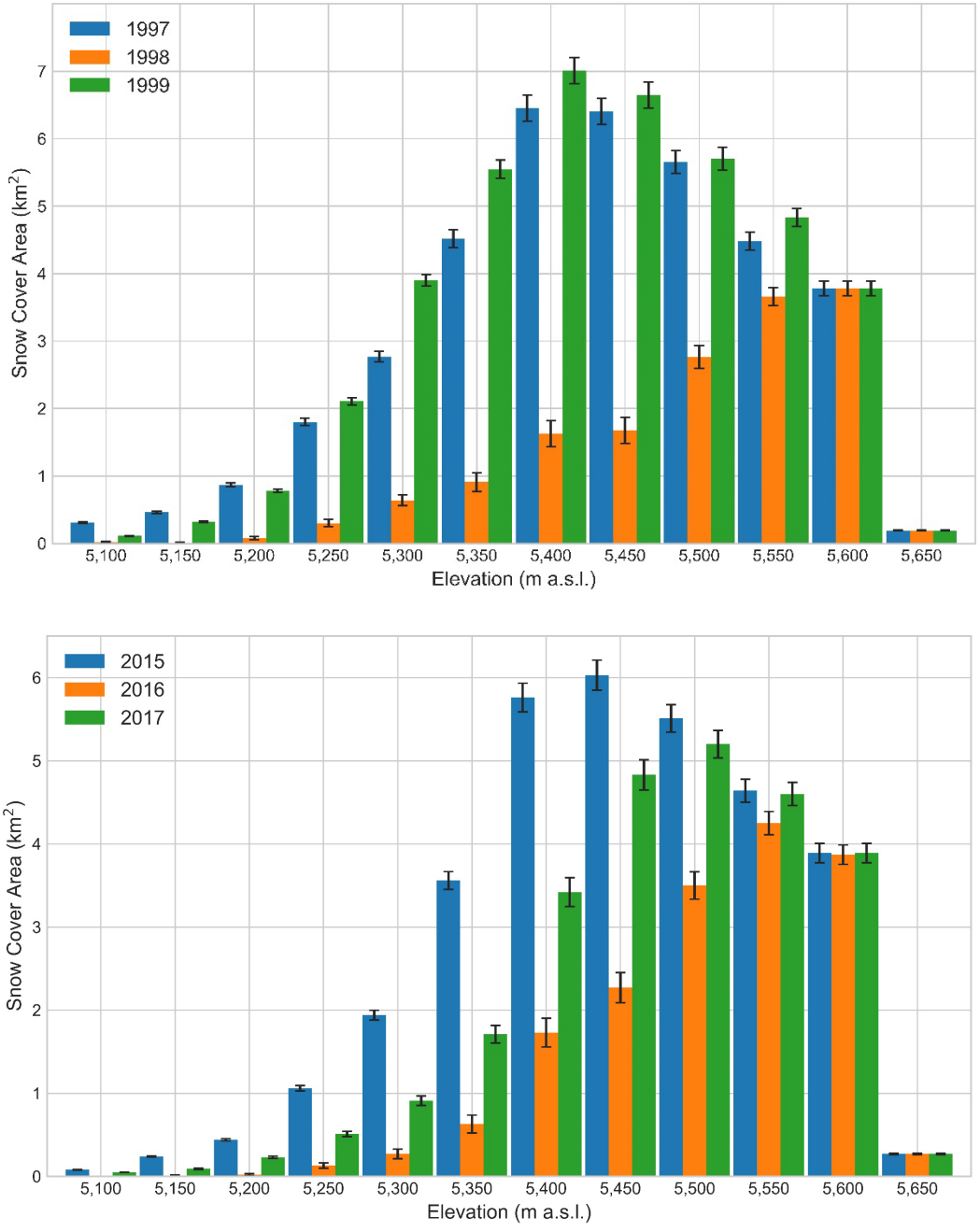

Figure 3: Percentage of snow cover displaying reduction~~loss~~ and rebound of the SCA during the 1998 El Niño event (top) and incomplete recovery following the 2016 El Niño event (bottom).

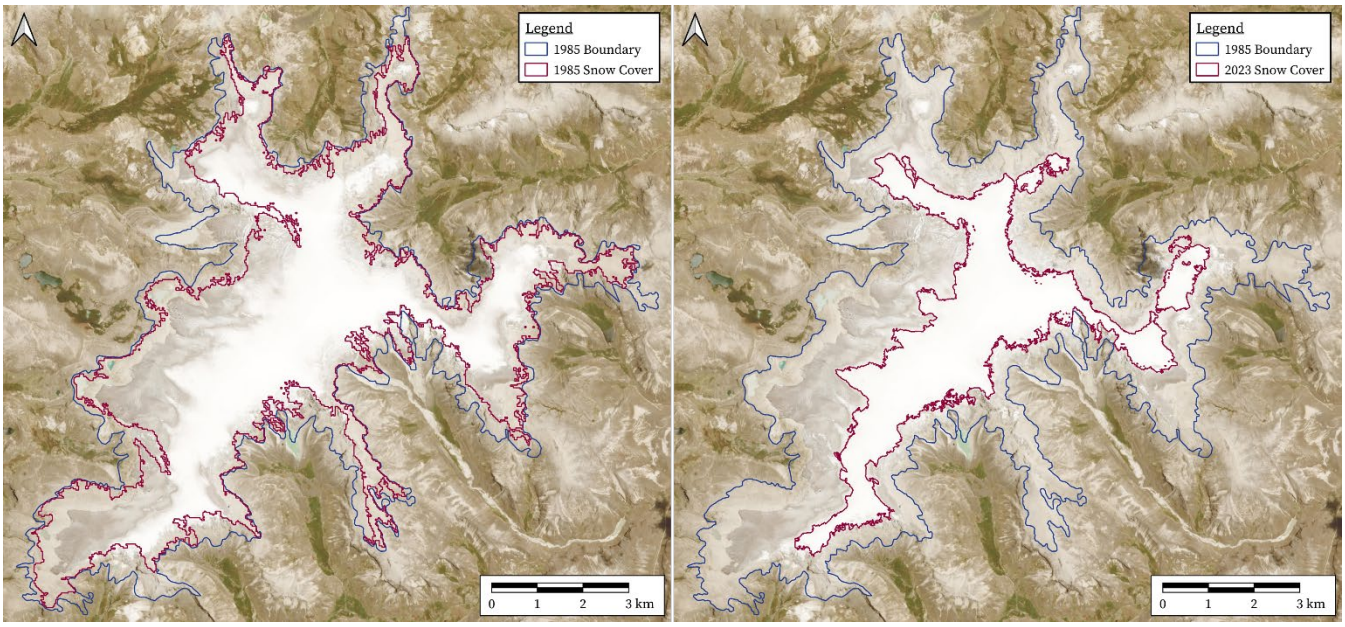

Figure 4: Decrease in the QIC's SCA (red) and TA (blue) at the end of the dry season from 1985 (left) to 2023 (right). Base Imagery obtained from Planet Labs Dove Satellite with 3-meter resolution, October 2023.

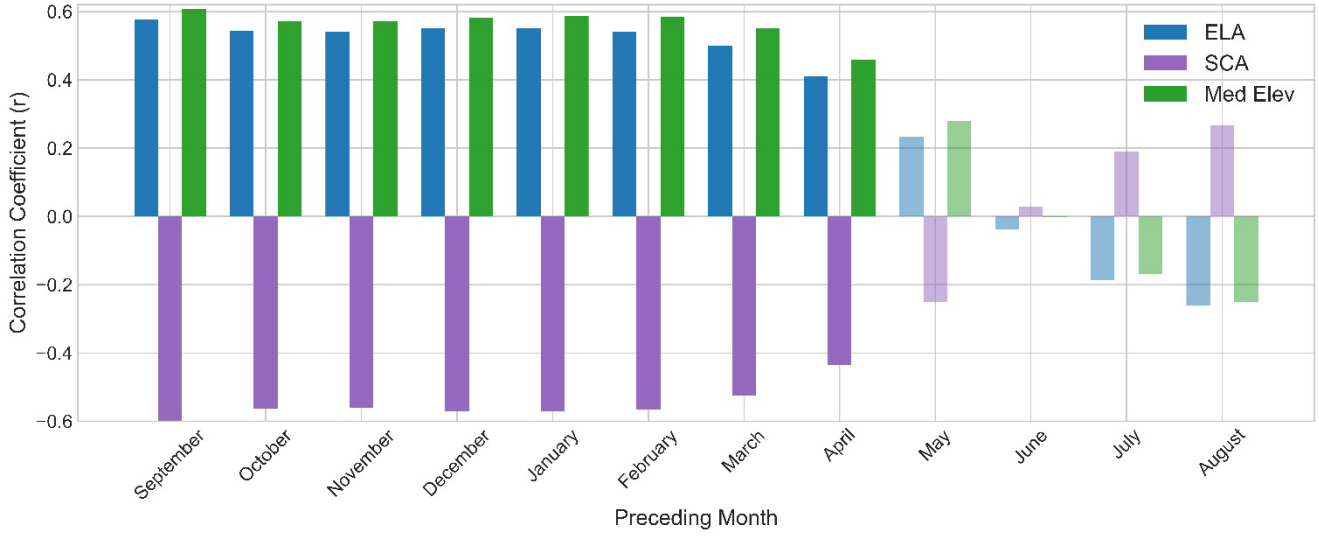

~~**Table**~~ **Figure 5~~1~~:** Zero-order correlations (*r*) for QIC variables (ELA, SCA, and Median Elevation (Med Elev)) and the ONI Index. Correlation coefficients with non-statistically significant p-values (>~~=~~0.05) are ~~indicated~~ denoted ~~in bold~~as semitransparent bars ~~italics~~.

4 Discussion

4.1 QIC Response to Short-Term Climate Variability

During El Niño events~~,~~ the Peruvian Andes are often drier than average (Sulca et al., 2018), with on-site measurements at Quelccaya recording warmer and drier conditions (J. Hurley et al., 2019). ~~Peru records higher precipitation along the northern coast, the Amazon, and the Andes (Lagos et al., 2008).~~ To be considered an El Niño event, the SST anomalies must be high for at least four consecutive months (Lagos et al., 2008). Our results suggest~~?~~ ~~, and it is likely that~~ these ~~longer term~~longer-term SST anomalies have a greater influence on the SCA than ~~singular~~ precipitation ~~events~~ (i.e., ~~, of which~~ no correlation is observed between wet season precipitation and the SCA, ELA, and SCA median elevation)~~, unlike the ONI index correlation~~. We ~~see~~ demonstrat~~ced evidence of these~~ that the El Niño events in 1998 and 2016 ~~impact~~correspond to~~ing~~ large reductions in QIC's~~the~~ SCA ~~and TA~~ (Fig. 6~~5~~). These SCA perturbations ~~record Z scores of -2.3 and -2.11,~~ are outliers from the ~~observed decline~~mean SCA (z-score= -2.3 and -2.11, respectively; avg z~~Z~~-score = 0.12). These~~, and~~ are evident in QIC shallow ice cores which display a 'smoothed' $\delta^{18}O$ signal during the El Niño instead of the usual high-resolution variability, indicating warm and dry conditions that lack accumulation and experience melt (Thompson et al., 2017). Linear r~~R~~egression analysis ~~completed~~ with and without El Niño event years~~s~~ show ~~record recorded~~ differing slope coefficients, indicating these events are associated with an enhanced reduction in~~ing the~~ QIC SCA~~ice loss~~~~reduction~~. As noted in the~~ the~~ results, the SCA rebound from the 2016 El Niño did not fully occur until years later, unlike in 1999 which was one of the strongest La Niña events (ONI Index of -1.5) within the observation period, along with 1989 and 2011.~~ ~~ This suggests the timing and magnitude of La Niña events are an additional factor influencing the year-to-year variability in SCA.

~~as 1999 (ONI Index of -1.5) was one of the strongest within the observation period, along with 1989 and 2011. In addition,cCorrelation during El Niño events between the monthly ELA and ONI index during El Niño events (1997-1999 and 2015-2017) declines arefrom 0.65 andto 0.34 , respectively. with respect to the 1998 and 2016 with the linear regression changing from an r-squared of 0.434 ($p<0.001$) to R^2r-squared of 0.12-07 ($p<0.0512$) El Niños.~~ If we consider El Niño and La Niña events that correspond~~ing~~ to ONI indexes greater than ±1.0, T~~t~~he linear regression model with ~~the~~ an El Niño binary predictor ~~records~~ shows a strong and significant relationship between TA and year ($R^2 = 0.94$, $p<0.001$). However,~~,~~ ~~but~~ variance ~~testing~~ analysis across the entire temporal scale indicates ~~the presence of~~that El Niño years have~~ provided~~ a stronger impact on~~to the~~ SCA, AAR, and ELA than on ~~the~~ TA (Fig. S4, Table S4~~5~~). While the SCA is notably briefly impacted by these El Niño events, decline from anthropogenic warming has resulted in the long-term decline of the SCA and TA of the QIC (Bradley et al., 2009; Rounce et al., 2023; Thompson et al., 2021; Vuille et al., 2018; Yarleque et al., 2018). Further, during all previously noted La Niña events (Fig. 6), the SCA experienced some level of temporary expansion, but throughout the 2021-2022 La Niña, the SCA did not ~~appear to~~ rebound, but only declined further. While this is only one incidence, we expect this behavior to continue through the onset of the predicted upcoming 2024/2025 ~~expected~~ La Niña. The decrease in the ~~percent~~ percentage of days at or below freezing during the wet season~~,~~ will only exacerbate the decline in SCA. In addition, a recent study has

~~indicated~~projected ~~th~~ ~~e expectation of~~ faster onset~~s~~ and slower decline ~~for~~ of future El Niños ~~future El Niños~~ (Lopez et al., 2022). ~~, and~~ C~~c~~onsidering the current state of the QIC and the ongoing El Niño, a slow decline ~~after~~ of the current event will only delay recovery of ~~in~~ the SCA, and act to enhance mass loss. ~~and continue to intensify its decline.~~

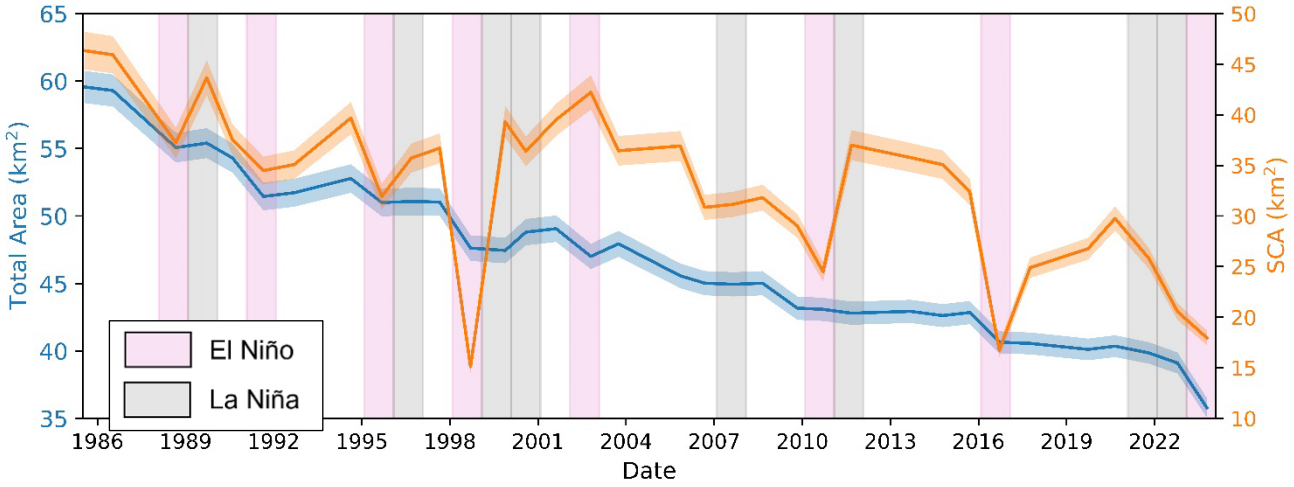

Figure 6~~5~~: Decline of QIC's TA and SCA over the observational period (1985-2023). Timing of El Niño and La Niña events (~~recording an~~with ONI indexes greater than ±1.0)~~-~~ are noted in pink and gray colored ~~coincide more readily with SCA than TA changes~~bars, respectively.~~.~~ ~~Strongest events are denoted with stars (*).~~

4.2 Equilibrium State of the QIC

Glaciers in other locations such as the New Zealand Alps and the European Alps are considered in steady state with AARs of around 0.6 (Benn & Lehmkuhl, 2000), but tropical glaciers require an AAR of ~0.8 (Kaser & Osmaston, 2002). Discounting El Niño years (1998, 2016, ~~&~~and 2023), the QIC average AAR is 0.744, indicating the QIC~~it~~ is out of equilibrium, and likely somewhat lagging in response compared with ~~with~~ the pace of ~~the~~ ongoing ~~changing~~ climate change. The ice cap is pushed even more noticeably out of equilibrium during the observed El Niño events with AARs of 0.310, 0.~~5~~41, and 0.5~~2~~3. These are far lower values than required for even high latitude glaciers, and far below the average for the QIC. Our results indicate t~~T~~he SCA has changed mor~~es more~~ dramatically on a year-to-year basis than the TA (Fig. 6~~5~~), ~~but the quick rebound of the AAR~~ indicating~~es~~ rapid response of the SCA and thus the ELA to short-term climate variability, in addition to~~and its more recent~~ decadal~~-~~-scale changes (Zekollari et al., 2020). This is consistent with other studies that indicate the~~e~~ QIC is likely responding to climate drivers within a few decades from the present, including the almost immediate response to El Niño events (Thompson, 2017; Veettil et al., 2017). Previous ~~analyses of~~work on Quelccaya ~~observed~~showed ~~T~~the median elevation of the entire QIC ~~was recorded rising~~rose ~1.59 m per decade from 1975 to 2010 (Taylor et al., 2022) ~~(Taylor et al., 2022)~~, which is slightly less than our~~this~~ estimate (~1.91 m/decade), ~~although~~ we note the different~~the~~ temporal scale ~~observed was different~~.

Similarly, previous studies of the QIC note a mean ELA between 1992 and 2017 of ~5,436 m a.s.l. (Yarleque et al., 2018) whileand our automated methods suggest a mean ELA of ~5,351 m a.s.l. for the same temporal scale. The QIC is likely responding to climate drivers within a few decades from the present, including the almost immediate response to El Niño events (Thompson, 2017; Veettil et al., 2017). This is evident in the regression analysis, when the El Niños are removed, the regression improves noticeably and variance testing to evaluate the mean of each variable during these different climatic conditionsConsidering the QIC's likely continuation of the out of equilibrium state, as well as projections continuing along the linearcontinued decline of the SCA and rise of the ELA due to ongoing anthropogenic climate change, we suggest indicate the possiblethat the QIC will lose its stop receiving snow coverSCA before 2080 (, becominge a wasting ice field) and may, and disappearance of the QICcompletely melt away by 2090prior to 2100 (assuming the rate of loss is constant; Fig. S5). FurtherHowever, with increasing ice loss, there is potential for an uneven ice surface with standing water to change the albedo, and thus affect the QIC's mass balance, enhancing its decline (Naegeli & Huss, 2017; Wang et al., 2015). As the ice continues to retreat, an uneven ice surface, future El Niños, and anthropogenic warming will likely exacerbate the process, pushing its demise closer to the present than expected.

5 Conclusion

We automate the process of satellite-based collection of yearly QIC parameters variables important for mass balance assessment and assess the ice cap's short-term fluctuations to local climate forcings, including temperature fluctuations and El Nino events. We observe and record decadal-scale change in TA, SCA, and ELA and high interannual variability in SCA and ELA. Specifically, we observe with staggering change in the QICloss over the last four decades including a ~42% TA loss in TA, a ~61% SCA loss in SCA, and a ~224 meter rise of the ELA. In the height of the wet season, the ONI index is the determining factosignificantlyr correlated with for the QIC's SCA at the's end of dry season, with noticeable decreases of the AAR during each El Niño event. While the SCA has responded rapidly to the ONI changes of the past, the SCA has declined through the most recent La Niña and is likelymay to continue to do so during the next. condition, but as anthropogenic warming continues to overwhelm natural climatic signals the entire SCA continues to rapidly decline. Continued monitoring of the QIC will be vital, as the potential for surface processes and future El Niños to accelerate the ice loss rises with continued warming. The implications forFurther, the QIC's future demise points towards water scarcity for the local population, creating uncharted difficulties alongside the lessening of a water source, especially seasonally (Veettil et al., 2017; Vuille et al., 2018). With ongoing warming, we expect to see continued shrinkage of both the SCA and the entire QIC in the coming decades.

Code and Data Availability

All calculated QIC variables from this study are provided within the supplementary information, detailed in Table S2. Annual SCA shapefile data and DEM bin distribution initially calculated within GEE is available at the following repository at https://doi.org/10.5281/zenodo.1126556810.5281/zenodo.10694300. A sample code for preprocessing and processing Landsat

8 images is available at the following url: ~~https://code.earthengine.google.com/72e85af2ec7e2e10482a939f7dd1cfe6?noload=true~~. https://code.earthengine.google.com/cfcbd0780ff3f09b0698035cd6dd678a.

Author Contribution

K.A.L. designed the study, developed the code, collected the snow cover data, and completed the analysis of the data and accompanying climate variables. K.A.L. wrote the manuscript. K.A.L., L.J.L, L.G.T., and B.G.M. contributed to the discussion of the results, editing, and revision of the manuscript.

Competing Interests

The authors declare that they have no conflict of interest.

Acknowledgments

This research was supported by the Heising-Simons Foundation and Volo Foundation for both past field data used as reference and in support of the current project. We would like to thank the National Science Foundation (NSF) for graduate student support under Award #1805819. Additionally, we thank James Lea for providing GEE assistance with topographic corrections, Rainey Aberle for providing guidance regarding ELA calculations, and Shelby Turner for insights into their climate projections in the Peruvian Andes. This is Byrd Polar and Climate Research Center contribution No. 1630.

References

Benn, D. I., & Lehmkuhl, F. (2000). Mass balance and equilibrium-line altitudes of glaciers in high-mountain environments. *Quaternary International*, *65*, 15–29.

Bradley, R. S., Keimig, F. T., Diaz, H. F., & Hardy, D. R. (2009). Recent changes in freezing level heights in the Tropics with implications for the deglacierization of high mountain regions. *Geophysical Research Letters*, *36*(17), 2009GL037712. https://doi.org/10.1029/2009GL037712

Bradley, R. S., Vuille, M., Diaz, H. F., & Vergara, W. (2006). Threats to water supplies in the tropical Andes. *Science*, *312*(5781), 1755–1756.

Braun, M. H., Malz, P., Sommer, C., Farías-Barahona, D., Sauter, T., Casassa, G., Soruco, A., Skvarca, P., & Seehaus, T. C. (2019). Constraining glacier elevation and mass changes in South America. *Nature Climate Change*, *9*(2), 130–136.

Brecher, H. H., & Thompson, L. G. (1993). Measurement of the Retreat of Qori Kalis Glacier in the Tropical Andes of Peru. *Terrestrial Photogrammetry*.

Casimiro, W.S.L., Labat, D., Ronchail, J., Espinoza, J. C., & Guyot, J. L. (2013). Trends in rainfall and temperature in the Peruvian Amazon–Andes basin over the last 40 years (1965–2007). *Hydrological Processes*, *27*(20), 2944–2957.

Dozier, J. (1989). Spectral signature of alpine snow cover from the Landsat Thematic Mapper. *Remote Sensing of Environment*, *28*, 9–22.

Ekstrand, S. (1996). Landsat TM-based forest damage assessment: Correction for topographic effects. *Photogrammetric Engineering and Remote Sensing*, *62*(2), 151–162.

Fang, H., Baiping, Z., Yonghui, Y., Yunhai, Z., & Yu, P. (2011). Mass Elevation Effect and Its Contribution to the Altitude of Snowline in the Tibetan Plateau and Surrounding Areas. *Arctic, Antarctic, and Alpine Research*, *43*(2), 207–212. https://doi.org/10.1657/1938-4246-43.2.207

Favier, V., Wagnon, P., & Ribstein, P. (2004). Glaciers of the outer and inner tropics: A different behaviour but a common response to climatic forcing. *Geophysical Research Letters*, *31*(16).

Gaddam, V. K., Boddapati, R., Kumar, T., Kulkarni, A. V., & Bjornsson, H. (2022). Application of "OTSU"—An image segmentation method for differentiation of snow and ice regions of glaciers and assessment of mass budget in Chandra basin, Western Himalaya using Remote Sensing and GIS techniques. *Environmental Monitoring and Assessment*, *194*(5), 337. https://doi.org/10.1007/s10661-022-09945-2

Ge, H., Lu, D., He, S., Xu, A., Zhou, G., & Du, H. (2008). Pixel-based Minnaert Correction Method for Reducing Topographic Effects on a Landsat 7 ETM+ Image. *Photogrammetric Engineering & Remote Sensing*, *74*(11), 1343–1350. https://doi.org/10.14358/PERS.74.11.1343

Hall, D. K., & Riggs, G. A. (2007). Accuracy assessment of the MODIS snow products. *Hydrological Processes*, *21*(12), 1534–1547.

Hanshaw, M. N., & Bookhagen, B. (2014). Glacial areas, lake areas, and snow lines from 1975 to 2012: Status of the Cordillera Vilcanota, including the Quelccaya Ice Cap, northern central Andes, Peru. *The Cryosphere*, *8*(2), 359–376. https://doi.org/10.5194/tc-8-359-2014

Hu, Z., Dietz, A., Zhao, A., Uereyen, S., Zhang, H., Wang, M., Mederer, P., & Kuenzer, C. (2020). Snow Moving to Higher Elevations: Analyzing Three Decades of Snowline Dynamics in the Alps. *Geophysical Research Letters*, *47*(12), e2019GL085742. https://doi.org/10.1029/2019GL085742

Hugonnet, R., McNabb, R., Berthier, E., Menounos, B., Nuth, C., Girod, L., Farinotti, D., Huss, M., Dussaillant, I., Brun, F., & Kääb, A. (2021). Accelerated global glacier mass loss in the early twenty-first century. *Nature*, *592*(7856), 726–731. https://doi.org/10.1038/s41586-021-03436-z

Hurley, J. V., Vuille, M., Hardy, D. R., Burns, S. J., & Thompson, L. G. (2015). Cold air incursions, δ^{18}O variability, and monsoon dynamics associated with snow days at Quelccaya Ice Cap, Peru. *Journal of Geophysical Research: Atmospheres*, *120*(15), 7467–7487. https://doi.org/10.1002/2015JD023323

Hurley, J., Vuille, M., & Hardy, D. R. (2019). On the interpretation of the ENSO signal embedded in the stable isotopic composition of Quelccaya Ice Cap, Peru. *Journal of Geophysical Research: Atmospheres*, *124*(1), 131–145.

Kaser, G., & Osmaston, H. (2002). *Tropical glaciers*. Cambridge University Press.

Klein, A. G., & Isacks, B. L. (1999). Spectral mixture analysis of Landsat thematic mapper images applied to the detection of the transient snowline on tropical Andean glaciers. *Global and Planetary Change*, *22*(1–4), 139–154. https://doi.org/10.1016/S0921-8181(99)00032-6

Lamantia, K., Thompson, L., Davis, M., Mosley-Thompson, E., & Stahl, H. (2023). Unique Collections of ^{14}C-Dated Vegetation Reveal Mid-Holocene Fluctuations of the Quelccaya Ice Cap, Peru. *Journal of Geophysical Research: Earth Surface*, *128*(11), e2023JF007297. https://doi.org/10.1029/2023JF007297

Li, X., Wang, N., & Wu, Y. (2022). Automated Glacier Snow Line Altitude Calculation Method Using Landsat Series Images in the Google Earth Engine Platform. *Remote Sensing*, *14*(10), 2377. https://doi.org/10.3390/rs14102377

Liu, C., Li, Z., Zhang, P., Tian, B., Zhou, J., & Chen, Q. (2021). Variability of the snowline altitude in the eastern Tibetan Plateau from 1995 to 2016 using Google Earth Engine. *Journal of Applied Remote Sensing*, *15*(04). https://doi.org/10.1117/1.JRS.15.048505

Lopez, H., Lee, S.-K., Kim, D., Wittenberg, A. T., & Yeh, S.-W. (2022). Projections of faster onset and slower decay of El Niño in the 21st century. *Nature Communications*, *13*(1), 1915.

Mark, B. G., Seltzer, G. O., Rodbell, D. T., & Goodman, A. Y. (2002). Rates of Deglaciation during the Last Glaciation and Holocene in the Cordillera Vilcanota-Quelccaya Ice Cap Region, Southeastern Perú. *Quaternary Research*, *57*(3), 287–298. https://doi.org/10.1006/qres.2002.2320

Meier, M. F. (1962). Proposed definitions for glacier mass budget terms. *Journal of Glaciology*, *4*(33), 252–263.

Naegeli, K., & Huss, M. (2017). Sensitivity of mountain glacier mass balance to changes in bare-ice albedo. *Annals of Glaciology*, *58*(75pt2), 119–129.

Paul, F., Barrand, N. E., Baumann, S., Berthier, E., Bolch, T., Casey, K., Frey, H., Joshi, S., Konovalov, V., & Le Bris, R. (2013). On the accuracy of glacier outlines derived from remote-sensing data. *Annals of Glaciology*, *54*(63), 171–182.

Pepin, N., Arnone, E., Gobiet, A., Haslinger, K., Kotlarski, S., Notarnicola, C., Palazzi, E., Seibert, P., Serafin, S., & Schöner, W. (2022). Climate changes and their elevational patterns in the mountains of the world. *Reviews of Geophysics*, *60*(1), e2020RG000730.

Pepin, N., Bradley, R. S., Diaz, H. F., Baraer, M., Caceres, E. B., Forsythe, H., Fowler, G., Greenwood, G., Hasmi, M. Z., Liu, X. D., Miller, J. R., Ning, L., Ohmura, A., Palazzi, E., Rangwala, I., Schöner, Severskiy, I., Shahgedanova, M., Wang, M. B., … Yang, D. Q. (2015). Elevation-dependent warming in mountain regions of the world. *Nature Climate Change*, *5*(5), 424–430.

Rabatel, A., Bermejo, A., Loarte, E., Soruco, A., Gomez, J., Leonardini, G., Vincent, C., & Sicart, J. E. (2012). Can the snowline be used as an indicator of the equilibrium line and mass balance for glaciers in the outer tropics? *Journal of Glaciology*, *58*(212), 1027–1036.

Rabatel, A., Francou, B., Soruco, A., Gomez, J., Cáceres, B., Ceballos, J. L., Basantes, R., Vuille, M., Sicart, J.-E., & Huggel, C. (2013). Current state of glaciers in the tropical Andes: A multi-century perspective on glacier evolution and climate change. *The Cryosphere*, *7*(1), 81–102.

Racoviteanu, A. E., Rittger, K., & Armstrong, R. (2019). An Automated Approach for Estimating Snowline Altitudes in the Karakoram and Eastern Himalaya From Remote Sensing. *Frontiers in Earth Science*, *7*, 220. https://doi.org/10.3389/feart.2019.00220

Rounce, D. R., Hock, R., Maussion, F., Hugonnet, R., Kochtitzky, W., Huss, M., Berthier, E., Brinkerhoff, D., Compagno, L., & Copland, L. (2023). Global glacier change in the 21st century: Every increase in temperature matters. *Science*, *379*(6627), 78–83.

Sankey, T., Donald, J., McVay, J., Ashley, M., O'Donnell, F., Lopez, S. M., & Springer, A. (2015). Multi-scale analysis of snow dynamics at the southern margin of the North American continental snow distribution. *Remote Sensing of Environment*, *169*, 307–319.

Schauwecker, S., Rohrer, M., Acuña, D., Cochachin, A., Dávila, L., Frey, H., Giráldez, C., Gómez, J., Huggel, C., Jacques-Coper, M., Loarte, E., Salzmann, N., & Vuille, M. (2014). Climate trends and glacier retreat in the Cordillera Blanca, Peru, revisited. *Global and Planetary Change*, *119*, 85–97. https://doi.org/10.1016/j.gloplacha.2014.05.005

Seehaus, T., Malz, P., Sommer, C., Soruco, A., Rabatel, A., & Braun, M. (2020). Mass balance and area changes of glaciers in the Cordillera Real and Tres Cruces, Bolivia, between 2000 and 2016. *Journal of Glaciology*, *66*(255), 124–136.

Sulca, J., Takahashi, K., Espinoza, J., Vuille, M., & Lavado-Casimiro, W. (2018). Impacts of different ENSO flavors and tropical Pacific convection variability (ITCZ, SPCZ) on austral summer rainfall in South America, with a focus on Peru. *International Journal of Climatology*, *38*(1), 420–435.

Taylor, L. S., Quincey, D. J., Smith, M. W., Potter, E. R., Castro, J., & Fyffe, C. L. (2022). Multi-Decadal Glacier Area and Mass Balance Change in the Southern Peruvian Andes. *Frontiers in Earth Science*, *10*.

Thompson, L. G. (2000). Ice core evidence for climate change in the Tropics: Implications for our future. *Quaternary Science Reviews*, *19*(1–5), 19–35. https://doi.org/10.1016/S0277-3791(99)00052-9

Thompson, L. G. (2017). Past, present, and future of glacier archives from the world's highest mountains. *Proceedings of the American Philosophical Society*, *161*(3), 226–243.

Thompson, L. G., Davis, M. E., Mosley-Thompson, E., Beaudon, E., Porter, S. E., Kutuzov, S., Lin, P. -N., Mikhalenko, V. N., & Mountain, K. R. (2017). Impacts of Recent Warming and the 2015/2016 El Niño on Tropical Peruvian Ice Fields. *Journal of Geophysical Research: Atmospheres*, *122*(23). https://doi.org/10.1002/2017JD026592

Thompson, L. G., Davis, M. E., Mosley-Thompson, E., Porter, S. E., Corrales, G. V., Shuman, C. A., & Tucker, C. J. (2021). The impacts of warming on rapidly retreating high-altitude, low-latitude glaciers and ice core-derived climate records. *Global and Planetary Change*, *203*, 103538. https://doi.org/10.1016/j.gloplacha.2021.103538

Thompson, L. G., Mosley-Thompson, E., Bolzan, J. F., & Koci, B. R. (1985). A 1500-Year Record of Tropical Precipitation in Ice Cores from the Quelccaya Ice Cap, Peru. *Science*, *229*(4717). https://doi.org/10.1126/science.229.4717.971

Thompson, L. G., Mosley-Thompson, E., Davis, M. E., & Brecher, H. H. (2011). Tropical glaciers, recorders and indicators of climate change, are disappearing globally. *Annals of Glaciology*, *52*(59), 23–34. https://doi.org/10.3189/172756411799096231

Thompson, L. G., Mosley-Thompson, E., Davis, M. E., Zagorodnov, V. S., Howat, I. M., Mikhalenko, V. N., & Lin, P.-N. (2013). Annually Resolved Ice Core Records of Tropical Climate Variability over the Past ~1800 Years. *Science*, *340*(6135). https://doi.org/10.1126/science.1234210

Veettil, B. K., Wang, S., Florêncio de Souza, S., Bremer, U. F., & Simões, J. C. (2017). Glacier monitoring and glacier-climate interactions in the tropical Andes: A review. *Journal of South American Earth Sciences*, *77*, 218–246. https://doi.org/10.1016/j.jsames.2017.04.009

Vuille, M., Bradley, R. S., & Keimig, F. (2000). Interannual climate variability in the Central Andes and its relation to tropical Pacific and Atlantic forcing. *Journal of Geophysical Research: Atmospheres*, *105*(D10), 12447–12460. https://doi.org/10.1029/2000JD900134

Vuille, M., Carey, M., Huggel, C., Buytaert, W., Rabatel, A., Jacobsen, D., Soruco, A., Villacis, M., Yarleque, C., Elison Timm, O., Condom, T., Salzmann, N., & Sicart, J.-E. (2018). Rapid decline of snow and ice in the tropical Andes – Impacts, uncertainties and challenges ahead. *Earth-Science Reviews*, *176*, 195–213. https://doi.org/10.1016/j.earscirev.2017.09.019

Vuille, M., Franquist, E., Garreaud, R., Lavado Casimiro, W. S., & Cáceres, B. (2015). Impact of the global warming hiatus on Andean temperature. *Journal of Geophysical Research: Atmospheres*, *120*(9), 3745–3757.

Vuille, M., Kaser, G., & Juen, I. (2008). Glacier mass balance variability in the Cordillera Blanca, Peru and its relationship with climate and the large-scale circulation. *Global and Planetary Change*, *62*(1–2), 14–28. https://doi.org/10.1016/j.gloplacha.2007.11.003

Wang, W., Xiang, Y., Gao, Y., Lu, A., & Yao, T. (2015). Rapid expansion of glacial lakes caused by climate and glacier retreat in the Central Himalayas. *Hydrological Processes*, *29*(6), 859–874.

Yarleque, C., Vuille, M., Hardy, D. R., Timm, O. E., De la Cruz, J., Ramos, H., & Rabatel, A. (2018). Projections of the future disappearance of the Quelccaya Ice Cap in the Central Andes. *Scientific Reports*, *8*(1), 1–11.

Zekollari, H., Huss, M., & Farinotti, D. (2020). On the imbalance and response time of glaciers in the European Alps. *Geophysical Research Letters*, *47*(2), e2019GL085578.